Comparisons of HELIOS Simulation Results Using PROPACEOS and SESAME Equations of State

In this brief memo, we discuss results from several benchmark calculations performed with the HELIOS radiation-hydrodynamics code to assess the accuracy of the equation of state (EOS) models in PROPACEOS. A summary of the modeling used in PROPACEOS is provided in Ref. [1]. To this end, we have run calculations that span a broad range of the EOS parameter space of several common materials. In each case, HELIOS simulation results computed using the PROPACEOS EOS tables are compared with those using SESAME EOS tables [2].

PROPACEOS uses a QEOS-type model [3] in the strong coupling regime (*i.e.*, at relatively high densities and low temperatures), and an isolated atom model which utilizes detailed atomic structure modeling in the weak coupling region. Properties between the weak and strong coupling regimes are obtained by interpolating in a thermodynamically consistent manner.

Below we discuss results from simulations using CH, Al, and Au, thereby spanning materials having a broad range of atomic number. The SESAME tables used in these calculations were tables 7590 for CH, 3717 for Al, and 2700 for Au.

1. Aluminum Flyer Plate Simulation

In this calculation, an 80 ns laser beam pulse, with a fluence of 50 J/cm^2 and wavelength of 1.06 μm, is used to accelerate an Al flyer plate (Figure 1). The flyer plate exhibits an initial rapid acceleration, and then reaches a steady speed. The system evolves at low temperatures and the flyer plate has nearly solid density throughout the calculation, making this a good test of the QEOS model in PROPACEOS.

Figure 2 shows the time-dependent velocity of a volume element just inside the flier plate (a depth of $\rho \Delta r$ = 4 x 10^{-3} g/cm^2). Note the good agreement between the results obtained using PROPACEOS and SESAME data both in the acceleration phase and in the oscillations at later time. The oscillations of the velocity can be interpreted as reverberations of the flying solid plate.

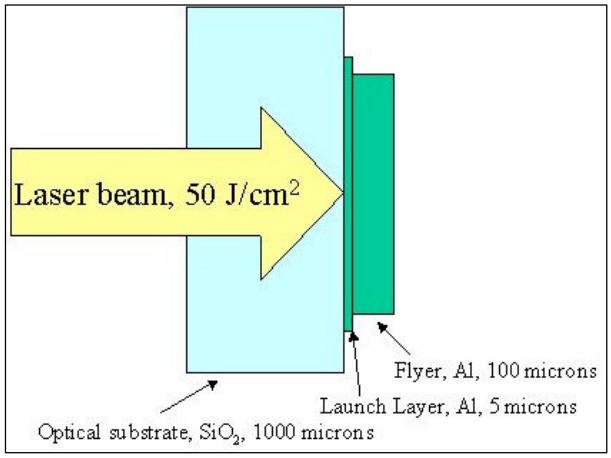

Figure 1. Schematic illustration of target setup in Al flyer plate calculation.

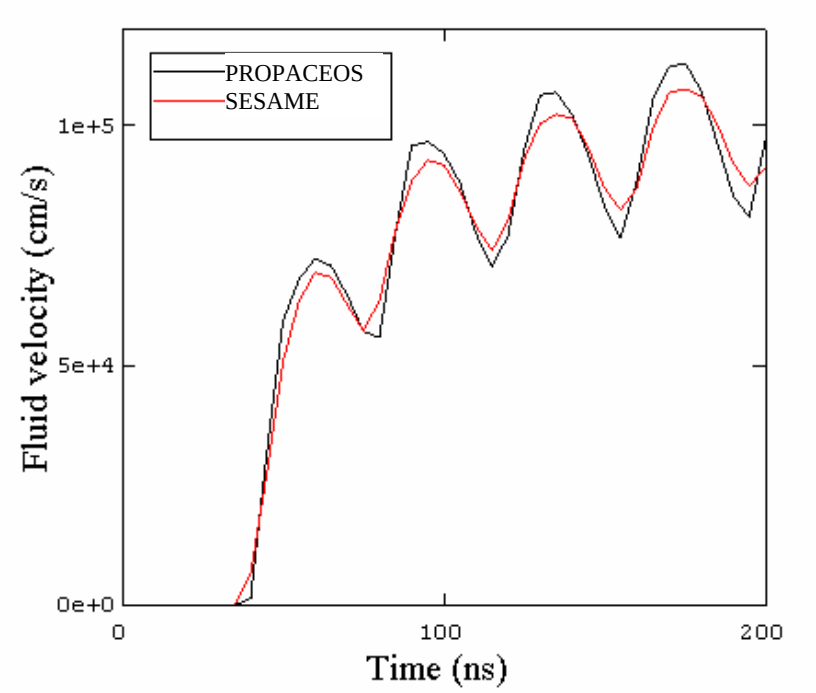

Figure 2. Velocity of a volume element just inside the flyer plate boundary vs. time for HELIOS calculations using PROPACEOS (black curve) and SESAME (red curve).

2. Radiation-Driven Shock in Al Foil

In this calculation, an external radiation source, with a peak radiation temperature of approximately 225 eV, drives a strong shock through an Al foil. As shown in Figure 3, the shock speed obtained using the PROPACEOS equation of state is essentially the same as that for the SESAME case. Figure 4 displays temperature and pressure profiles 2 ns after the irradiation starts. Temperatures and pressures are sensitive to the details of the equation of state and the profiles show little difference between the PROPACEOS and SESAME data.

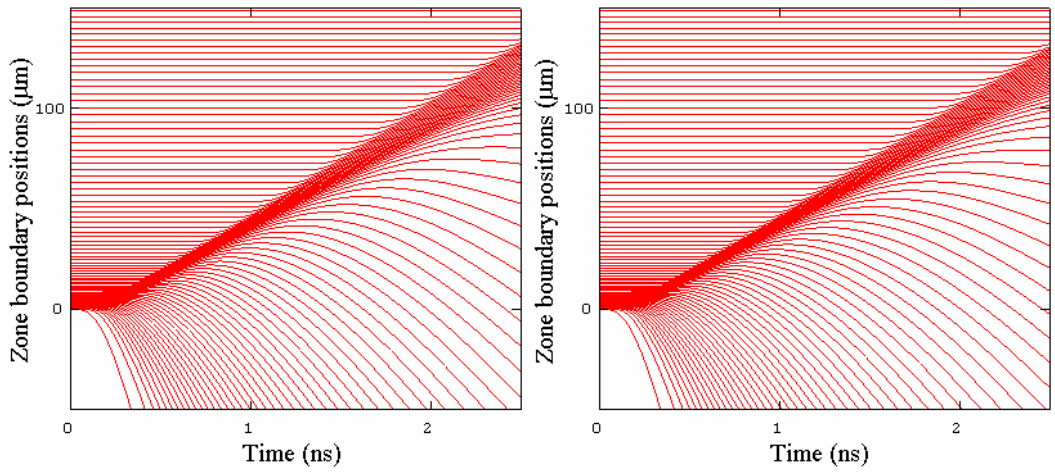

Figure 3. Lagrangian zone boundary positions in HELIOS simulation of an Al foil heated on one side by an intense radiation field. Left: PROPACEOS results. Right: SESAME results.

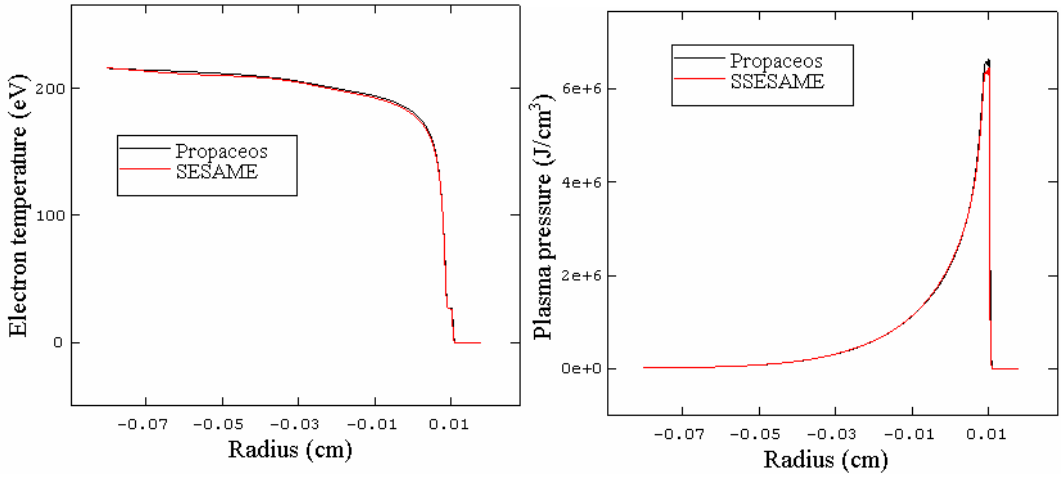

Figure 4. Al plasma temperature and pressure profiles at 2 ns.

3. Radiation-Driven Shock in Planar CH Sample

This calculation uses the same parameters as the one discussed in the previous section, but in this case the material being heated is CH. Figures 5 and 6 show results for the time-dependent Lagrangian zone boundary positions and the temperature and density profiles at t = 2 ns. The shock speed is significantly higher compared with the aluminum case. The agreement between the calculations using SESAME and PROPACEOS equation of state data is again seen to be very good.

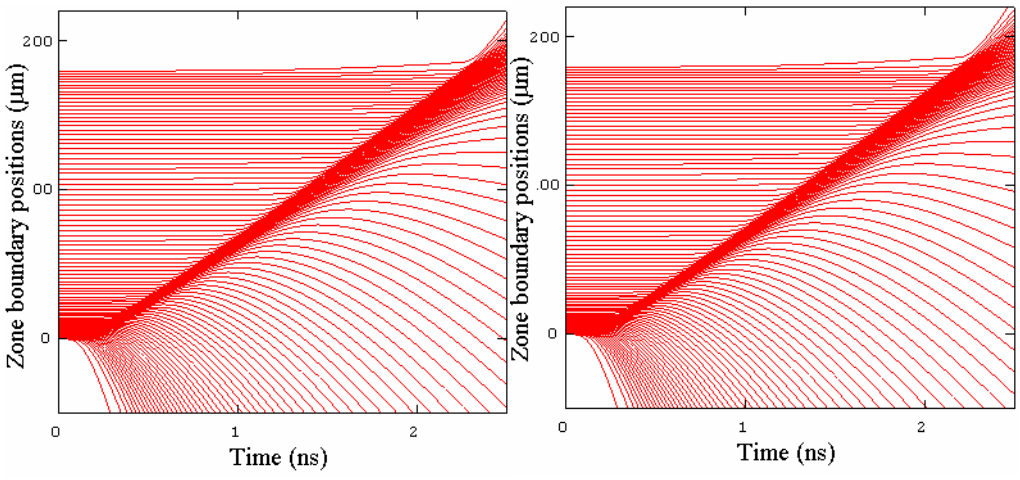

Figure 5. Lagrangian zone boundary positions in HELIOS simulation of a planar CH sample heated on one side by an intense radiation field. Left: PROPACEOS results. Right: SESAME results.

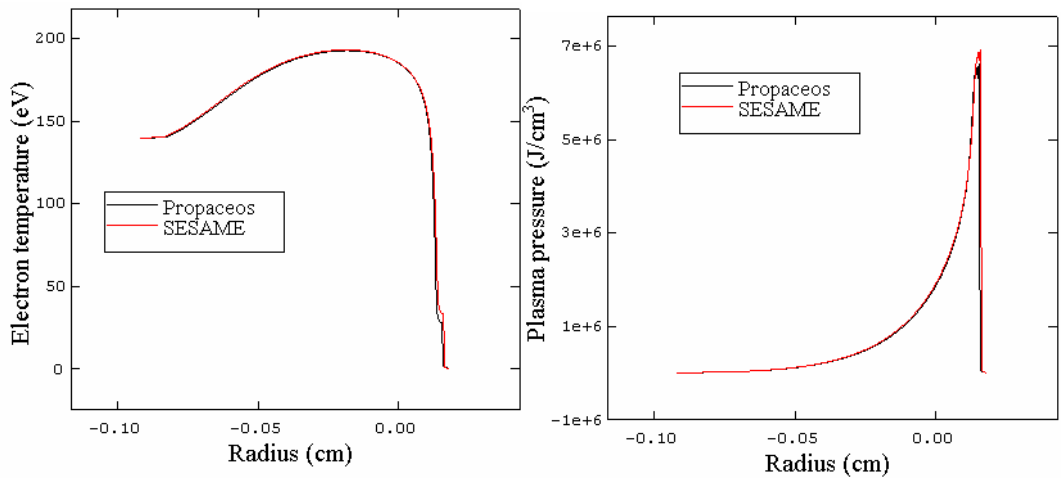

Figure 6. CH plasma temperature and pressure profiles at 2 ns.

4. Radiation-Driven Shock in a Gold Foil

This calculation uses the same parameters as the one discussed in the previous two sections, but in this case a thin gold (Au) foil is heated. Figures 7 and 8 summarize the results. The shock speed is significantly lower compared with the aluminum case. The agreement between the calculations using SESAME and PROPACEOS equation of state data is again seen to be very good. Thus, good agreement has been shown over a wide span of material atomic number.

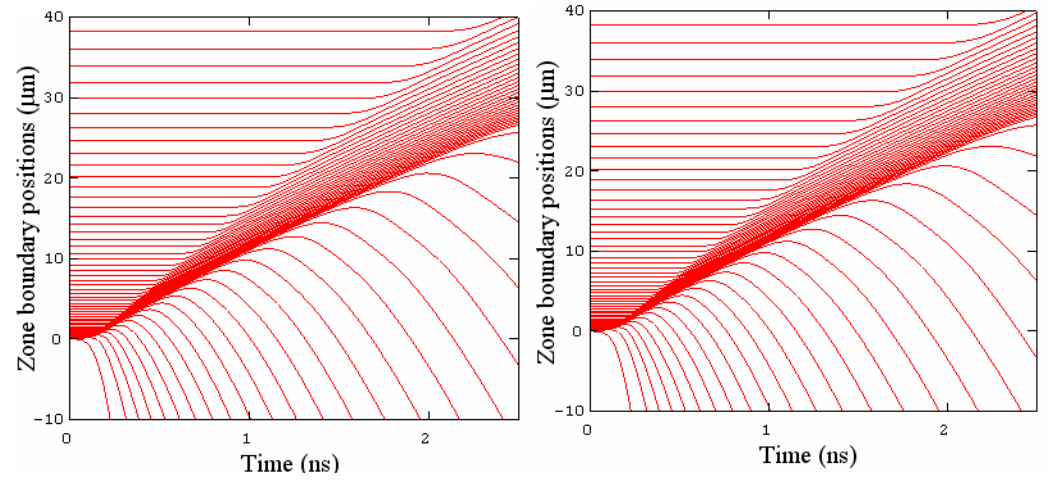

Figure 7. Lagrangian zone boundary positions in HELIOS simulation of a planar Au foil heated on one side by an intense radiation field. Left: PROPACEOS results. Right: SESAME results.

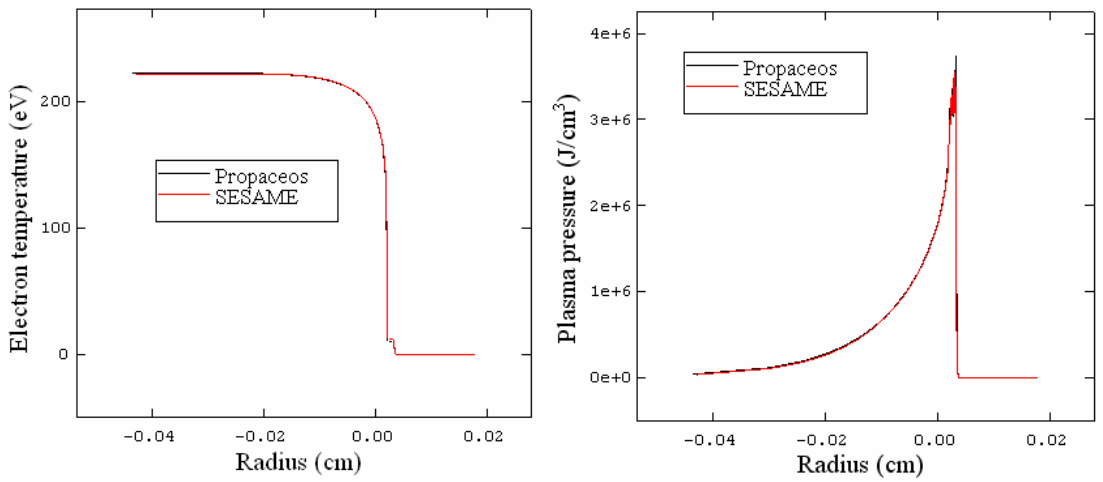

Figure 8. Au plasma temperature and pressure profiles at 2 ns.

5. Radiation-Driven Capsule Implosion

In this calculation, a plastic micro balloon, with a wall thickness of 35 μm and an internal diameter of 220 μm, is filled with 50 atm DD. The capsule is driven by 200 eV radiation for 1 ns. This system is representative of the indirectly driven capsule implosion experiments at OMEGA. The calculation is an integrated test of several physics modules. The implosion performance depends strongly on the timing of the shocks and therefore on the details of the EOS. Figure 9 shows good agreement for the radiation power at the surface of the capsule as a function of time. The neutron yield, however, is seen to be somewhat higher in the calculation performed using the SESAME EOS (Figure 10). This neutron yield is very sensitive to the conditions obtained in the implosion core, and thus small differences in the shock properties can lead to more noticeable differences in the neutron yield.

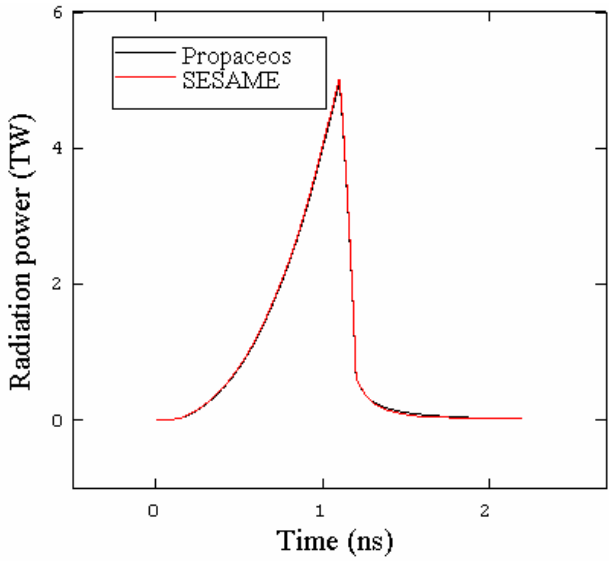

Figure 9. Radiation power emitted at the outer boundary of the capsule.

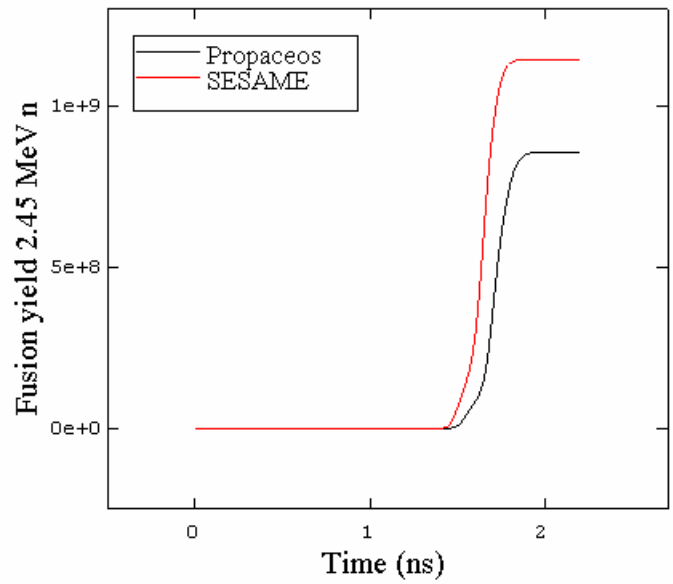

Figure 10. Time-integrated 2.45 MeV neutron yield as a function of time.

The neutron production starts earlier and results in higher fusion yield when SESAME tables are used. The likely explanation of this behavior is that the shock speed is slightly higher for the calculations with SESAME tables. When the main shock collapses at the target center, the temperatures rise quickly and neutrons are generated. This can also be seen in Figure 11 which shows electron and ion temperatures in the innermost zone as a function of time.

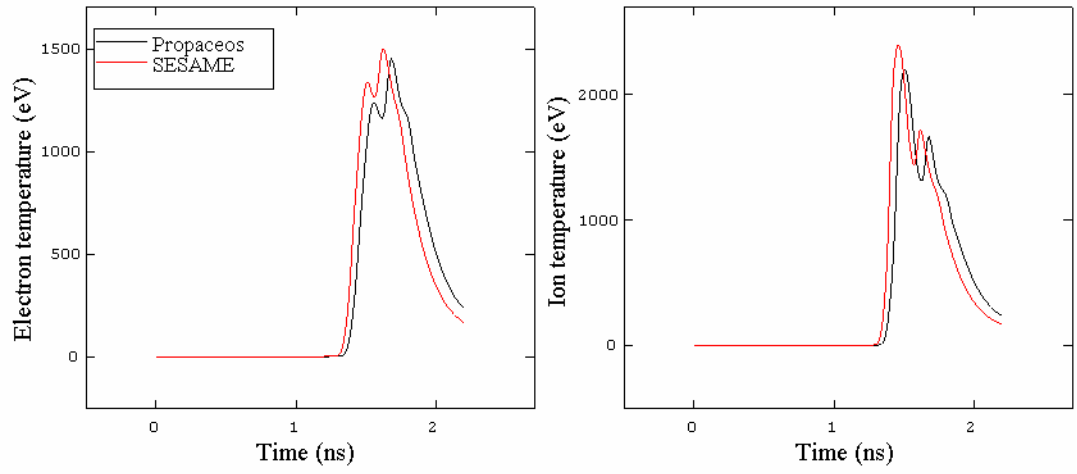

Figure 11. Time histories of the electron and ion temperatures at the center of the core.

6. Summary

HELIOS simulations performed using PROPACEOS equations of state for CH, Al, and Au show very good agreement with results computed using SESAME tables. A series of simulations, which access a broad range of temperature and density space, were performed to assess the reliability of the PROPACEOS equation of state. The good agreement between the PROPACEOS and SESAME results suggest the PROPACEOS equation of state, at least for the parameter space addressed in this memo, should be reliable.

References

[1] J. J. MacFarlane, I. E. Golovkin, and P. R. Woodruff, "*HELIOS-CR – A 1-D Magnetohydrodynamics Code with Inline Atomic Kinetics Modeling*," J. Quant. Spectrosc. Rad. Tranfer, **99**, 381 (2006).

[2] S. P. Lyon, and J. D. Johnson, "*SESAME: The Los Alamos National Laboratory Equation of State Database*," LANL Technical Report LA-UR-92-3407, Los Alamos National Laboratory, Los Alamos, NM (1992).

[3] R. M. More, K. H. Warren, D. A. Young, and G. B. Zimmerman, "*A New Quotidian Equation of State (QEOS) for Hot Dense Matter*," Phys Plasmas **31**, 3059 (1988).